Hypothetical Thermodynamic Properties: Vapor Pressures and Vaporization Enthalpies of the Even *n*-Alkanes from C_{78} to C_{92} at $T = 298.15$ K by Correlation−Gas Chromatography

James Chickos* and Dmitry Lipkind

Department of Chemistry and Biochemistry, University of Missouri−St. Louis, St. Louis, Missouri 63121

The temperature dependence of gas chromatographic retention times of hexaheptacontane to dononacontane is reported. These data are used with a summary of earlier work to evaluate and compare the vaporization enthalpies and vapor pressures of the *n*-alkanes from $T = (298.15$ to $540)$ K for heneicosane to dononacontane. The vapor pressure and vaporization enthalpy results obtained are compared with estimated data from Morgan's "PERT2" extended corresponding states principle (CSP) which uses *n*-alkane input parameters based on the works of Kudchadker and Zwolinski and of Tsu. The results are also compared with a model previously developed from empirical data which predicts that vaporization enthalpies measured at the boiling temperatures should approach a maximum value and then asymptotically approach zero as the chain length approaches infinity. Some curvature in the enthalpy of transfer from the gas chromatographic column to the gas phase, expected to show the same dependence on size, is indeed observed as the number of carbon atoms exceeds 60. The vapor pressure equations generated from the gas chromatographic results are used to predict boiling temperatures. A comparison of these temperatures with those obtained by extrapolation of an empirical fit of experimental boiling temperatures to a hyperbolic function is remarkably good.

Introduction

The *n*-alkanes serve as excellent standards for the measurement of vaporization enthalpies of hydrocarbons at $T = 298.15$ K, regardless of the physical state of the hydrocarbon.[1−4] Recently, we have reported the vaporization enthalpies of the even hydrocarbons, tetracontane to hexaheptaconane (C_{40} to C_{76}), and described a protocol that could be used to evaluate the subcooled liquid vapor pressure values of these materials.[5] Equations were reported that are capable of reproducing the vapor pressures of the liquid state of these materials from $T = (298.15$ to $540)$ K. There are no experimental vapor pressures available for these large molecules for comparison. Experimental vaporization enthalpies and vapor pressures for molecules larger than heneicosane are scarce, and all the values cited in this work have been generated by extrapolation of recommended vaporization enthalpies and vapor pressure values[6] of the *n*-alkanes of C_{20} and smaller using the technique of correlation−gas chromatography. In instances where the results obtained by this technique could be directly compared to experimental values, the comparisons have been very good.[1,2,5]

Subcooled liquid vapor pressures and vaporization enthalpies of the larger *n*-alkanes are excellent standards for the evaluation of vaporization enthalpies and liquid vapor pressures of other hydrocarbons.[3,4,7,8] This work expands vaporization enthalpy and vapor pressure data available for the even alkanes from octaheptacontane to dononacontane and summarizes the results obtained for heneicosane to dononacontane. It also examines indirectly if the magnitude of the vaporization enthalpy at $T = 298.15$ K does show curvature with size as suggested by the apparent convergence of the normal boiling and critical temperatures.[9] Additionally, the experimental enthalpies of transfer as measured by gas chromatography are correlated with the

predictions of a computer program developed to model the vaporization enthalpies of the larger *n*-alkanes. Finally, the boiling temperatures predicted from the vapor pressure equations that result from the vapor pressure evaluations are used to predict hypothetical boiling temperatures of the larger *n*-alkanes. The results are compared to predictions of a hyperbolic function previously reported to model available experimental boiling temperatures.

The lack of experimental data for molecules of the size of this study has prompted us to compare our results to predictions based on the PERT2 corresponding states principle (CSP) methods of Morgan and Kobayashi[10,11] which have been included in a program called "PERT2". This program has input parameters for *n*-alkanes up to C_{100} which are based on the normal boiling temperature and Antoine constant correlations of Kudchadker and Zwolinski.[13] Antoine constants for the *n*-alkanes up to C_{100} along with their range of applicability have also been reported by Stephenson and Malanowski.[15] These constants are reproductions of constants reported by Kudchadker and Zwolinski[13] in different units, T/K and p/kPa rather than $t/°C$ and $p/mmHg$. The temperature limits reported by Stephenson and Malanowski correspond to calculated vapor pressures in the approximate range $(0.1$ to $101)$ kPa.

As observed previously,[5] the values obtained by correlation−gas chromatography for both vapor pressure and vaporization enthalpy were in very good agreement with the predictions of PERT2 and the extrapolations of Kudchadker and Zwolinski up to about hexacontane. As the number of carbon atoms increased above 60, the predictions of PERT2 and those of Kudchadker and Zwolinski began to increase less readily than the values obtained by correlation−gas chromatography, even though the results obtained by correlation−gas chromatography also began to show evidence of some curvature. This study expands the range of compounds studied, and current indications

---

* Corresponding author. E-mail: jsc@umsl.edu. Phone: 314 516 5377.
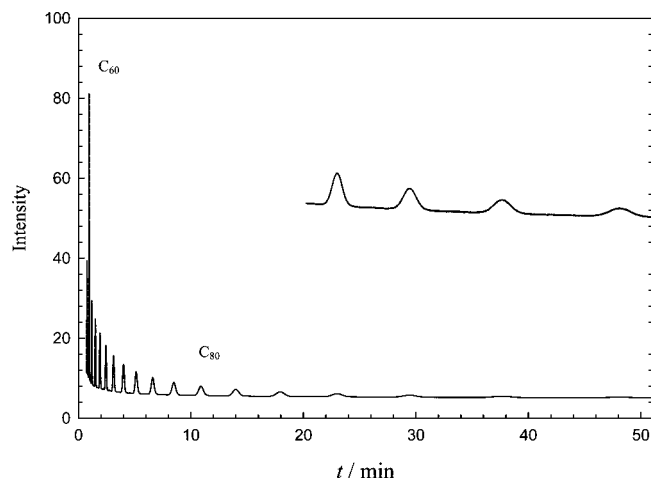
Figure 1. GC trace of Polywax1000 spiked with *n*-alkanes *n*-C$_{50}$ and *n*-C$_{60}$ at $T = 661$ K (run 1). The solvent peak and C$_{50}$ are not shown.
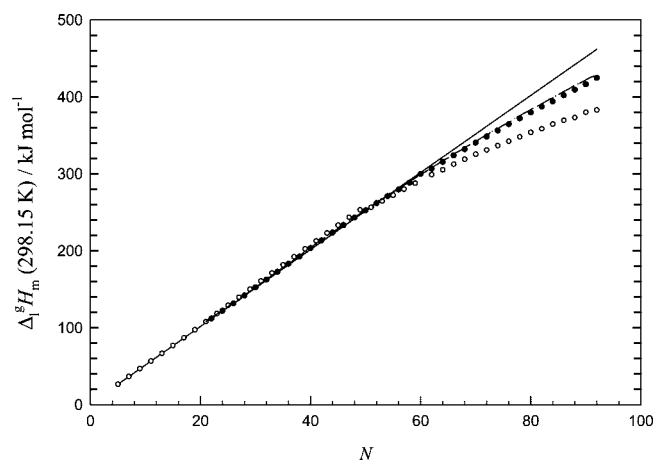
Figure 2. Vaporization enthalpies at $T = 298.15$ K for pentane to dononacontane. N represents the number of carbon atoms. The solid line was derived using the recommended vaporization enthalpies of pentane to eicosane (eq 4).[6] The empty circles are values calculated using the program PERT2 for the odd alkanes from pentane to nonapentcontane and the even alkanes from dohexacontane to dononacontane.[11] The solid circles are values evaluated from correlations of $\Delta_{sln}^g H_m(T_m)$ with $\Delta_l^g H_m(298.15$ K$)$ in this and previous studies.[1,2,5] The vaporization enthalpies indicated by the dashed line were calculated using the vapor pressures calculated from eq 9 and the constants of Table 4.

indicate that vaporization enthalpies do show continuing curvature with increasing size, although the experimental results suggest that the curvature observed with increasing carbon number is somewhat less than predicted by earlier models.

Experimental

Pentacontane and hexacontane were purchased from Aldrich from the Analytical Standards catalog. All the remaining alkanes studied up to C$_{94}$ were obtained as a mixture present in Polywax 1000 purchased from Restek Corporation. Polywax 1000 is an oligomer of polyethylene with an average molecular weight of 1000 g·mol^{-1}. The material consists of a series of even hydrocarbons, in which the C$_{40}$ to C$_{60}$ region contained compounds with identical retention times with *n*-alkanes purchased separately. A typical plot of Polywax 1000 spiked with C$_{50}$ and C$_{60}$ is shown in Figure 1. At the temperature used for this figure, necessary to observe the largest hydrocarbons of this study, the retention time of C$_{50}$ is obscured by the solvent and the other hydrocarbons present. Correlation gas chromatography experiments were performed on an HP 5890 gas

chromatograph equipped with a split/splitless capillary injection port and a flame ionization detector run at a split ratio of approximately 50/1. Retention times were rounded to three significant figures following the decimal point using HP software interfaced to a computer. The instrument was run isothermally using two high temperature aluminum clad silica capillary columns (0.25 mm ID, 0.01 μm methyl silicone film thickness, Quadex Corp., Catalog # 400 1HT-15-0.1F, 15 m; SGE Forte GC capillary column, 12 m × 0.32 mm ID). The injection temperature was maintained constant at the instrument's maximum of $T = 673$ °C, and the detector temperature was maintained at $T = 673$ K for runs 1 and 3 and $T = 693$ K for run 2. Helium was used as the carrier gas. At the temperatures of the experiments, the retention time of the solvent used, octane or toluene, was used as the nonretained reference. The retention times of the solvent were used to determine the dead volume of the column. Adjusted retention times, t_a, were calculated by subtracting the measured retention time of the solvent from the retention time of each analyte as a function of temperature over a 30 K range at 5 K intervals. The adjusted retention time measured by gas chromatography, t_a, is inversely proportional to the vapor pressure of an analyte on the column. A plot of $\ln(t_o/t_a)$ versus $1/T$, where t_o refers to the reference time, 1 min, results in a linear relationship in which the slope of the line is related to the enthalpy of transfer of an analyte off the column divided by the gas constant. Column temperatures were controlled by the gas chromatograph and were monitored independently by using a Fluke digital thermometer. Temperature was maintained constant by the instrument to ± 0.1 K. All plots of $\ln(t_o/t_a)$ vs $1/T$ were characterized with correlation coefficients, r^2, > 0.99. The retention times measured are reported as Supporting Information. To determine if the inability to adjust the injector above $T = 673$ K had any effect on the measured retention times, run 3 was run at column temperatures below $T = 673$ K, $T = (638$ to $668)$ K. The vaporization enthalpies obtained in this run were within experiment error of those obtained at higher temperatures (see Table 2 and Figure 3). In addition, values of t_o/t_a calculated from runs 1 to 3 were roughly within experimental error of each other (see Table 5).

Results

A. Vaporization Enthalpies. Experimental retention times are provided as Supporting Information. A plot of $\ln(t_o/t_a)$ vs $1/T$ resulted in linear plots whose slopes and intercepts are provided in Table 1 for three runs. The second and third columns of each section of Table 1 list the slopes and intercepts obtained from plots of $\ln(t_o/t_a)$ vs $1/T$. Enthalpies of transfer from the stationary phase of the column to the gas phase at the mean temperature T_m, $\Delta_{sln}^g H_m(T_m)$, were calculated by multiplying the slope of the line by the gas constant, $R = 8.314·10^{-3}$ kJ·mol^{-1}·K^{-1}, and by (-1), and are reported in column 4. Vaporization enthalpies evaluated previously for the even *n*-alkanes, pentacontane to hexaheptacontane,[5] are reported as standards in column 5 of Table 1 for three runs. The last column reports the vaporization enthalpies calculated from the correlation equation listed below each run, eqs 1 to 3. The vaporization enthalpies and their mean value are summarized in Table 2. The uncertainties reported in Table 1 are standard errors calculated from the uncertainty associated with the slopes and intercepts of eqs 1 to 3. The uncertainty reported for the mean in Table 2 is an average of the uncertainties of each run.

The vaporization enthalpies of all *n*-alkanes in the literature[1,2,15] from pentane to eicosane along with the results of these sets of extrapolations are summarized in Table 3 and illustrated in

Table 1. Enthalpies of Transfer and Vaporization Enthalpies Obtained for the Even *n*-Alkanes From Pentacontane to Dononacontane

run 1	slope (T/K)	intercept	$\Delta_{sln}^{g}H_m(676\ K)$ kJ·mol^{-1}	$\Delta_l^{g}H_m(298.15\ K)$ kJ·mol^{-1} (lit.)[5]	$\Delta_l^{g}H_m(298.15\ K)$ kJ·mol^{-1} (calcd)
pentacontane	−14177	23.047	117.862	252.5	254.6
dopentacontane	−14507	23.277	120.603	261.8	259.9
tetrapentacontane	−15180	24.022	126.204	271.0	270.8
hexapentacontane	−15851	24.763	131.779	279.7	281.6
octapentacontane	−16308	25.187	135.581	288.5	288.9
hexacontane	−16862	25.755	140.182	299.9	297.9
dohexacontane	−17397	26.299	144.628	306.8	306. 5
tetrahexacontane	−17919	26.824	148.970	315.4	314.9
hexahexacontane	−18449	27.364	153.381	324.0	323. 5
octahexacontane	−18968	27.887	157.695	331.9	331.8
heptacontane	−19487	28.411	162.006	340.3	340.2
doheptacontane	−20005	28.935	166.314	348.4	348.5
tetraheptacontane	−20501	29.429	170.439	356.2	356.5
hexaheptacontane	−21031	29.973	174.848	364.3	365.1
octaheptacontane	−21512	30.445	178.843		372.8 ± 3.4
octacontane	−22009	30.942	182.971		380.8 ± 3.5
dooctacontane	−22481	31.406	186.896		388.4 ± 3.6
tetraoctacontane	−22935	31.842	190.671		395.8 ± 3.6
hexaoctacontane	−23424	32.331	194.734		403.6 ± 3.7
octaoctancontane	−23898	32.801	198.677		411.3 ± 3.8
nonacontane	−24371	33.269	202.613		418.9 ± 3.9
dononacontane	−24814	33.695	206.291		426.0 ± 3.9

$$\Delta_l^{g}H_m(298.15\ K)/kJ\cdot mol^{-1} = (1.939 \pm 0.018)\Delta_{sln}^{g}H_m(676\ K) - (26.07 \pm 1.20)\quad r^2 = 0.9990 \quad (1)$$

run 2	slope (T/K)	intercept	$\Delta_{sln}^{g}H_m(676\ K)$ kJ·mol^{-1}	$\Delta_l^{g}H_m(298.15\ K)$ kJ·mol^{-1} (lit.)[5]	$\Delta_l^{g}H_m(298.15\ K)$ kJ·mol^{-1} (calcd)
octapentacontane	−15979	24.825	132.845	288.5	289.5
hexacontane	−16538	25.404	137.492	299.9	298.1
dohexacontane	−17131	26.037	142.420	306.8	307.2
tetrahexacontane	−17686	26.614	147.037	315.4	315.7
hexahexacontane	−18235	27.182	151.597	324.0	324.1
octahexacontane	−18763	27.722	155.990	331.9	332.2
heptacontane	−19287	28.256	160.345	340.3	340.2
doheptacontane	−19830	28.819	164.857	348.4	348.5
tetraheptacontane	−20338	29.334	169.085	356.2	356.3
hexaheptacontane	−20844	29.844	173.285	364.3	364.0
octaheptacontane	−21347	30.353	177.470		371.8 ± 3.4
octacontane	−21828	30.829	181.467		379.1 ± 3.5
dooctacontane	−22282	31.269	185.247		386.1 ± 3.6
tetraoctacontane	−22783	31.775	189.407		393.8 ± 3.6
hexaoctacontane	−23272	32.269	193.474		401.2 ± 3.7
octaoctancontane	−23779	32.789	197.688		409.0 ± 3.8
nonacontane	−24189	33.166	201.099		415.3 ± 3.9
dononacontane	−24684	33.669	205.214		422.9 ± 3.9

$$\Delta_l^{g}H_m(298.15\ K)/kJ\cdot mol^{-1} = (1.843 \pm 0.019)\Delta_{sln}^{g}H_m(676\ K) - (44.69 \pm 0.77)\quad r^2 = 0.9992 \quad (2)$$

run 3	slope (T/K)	intercept	$\Delta_{sln}^{g}H_m(653\ K)$ kJ·mol^{-1}	$\Delta_l^{g}H_m(298.15\ K)$ kJ·mol^{-1} (lit.)[5]	$\Delta_l^{g}H_m(298.15\ K)$ kJ·mol^{-1} (calcd)
hexacontane	−17713	26.912	147.261	299.9	298.5
dohexacontane	−18308	27.559	152.202	306.8	307.2
tetrahexacontane	−18897	28.197	157.099	315.4	315.8
hexahexacontane	−19480	28.827	161.946	324.0	324.4
octahexacontane	−20037	29.42	166.580	331.9	332.5
heptacontane	−20622	30.054	171.440	340.3	341.1
doheptacontane	−21090	30.515	175.336	348.4	347.9
tetraheptacontane	−21639	31.097	179.902	356.2	356.0
hexaheptacontane	−22169	31.652	184.305	364.3	363.7
octaheptacontane	−22708	32.222	188.782		371.6 ± 4.1
octacontane	−23197	32.717	192.850		378.7 ± 4.1
dooctacontane	−23768	33.338	197.595		387.1 ± 4.2
tetraoctacontane	−24146	33.666	200.742		392.6 ± 4.3
hexaoctacontane	−24753	34.345	205.789		401.5 ± 4.4
octaoctancontane	−25156	34.714	209.137		407.4 ± 4.5
nonacontane	−25678	35.265	213.475		415.0 ± 4.6

$$\Delta_l^{g}H_m(298.15\ K)/kJ\cdot mol^{-1} = (1.759 \pm 0.021)\Delta_{sln}^{g}H_m(653\ K) - (39.49 \pm 0.76)\quad r^2 = 0.9990 \quad (3)$$

Table 2. Summary of the Vaporization Enthalpies (in $kJ \cdot mol^{-1}$) of the Even Alkanes from Octaheptacosane to Dononacosane

|	run 1	run 2	run 3	average
octaheptacontane	372.8 ± 3.4	371.8 ± 3.6	371.6 ± 4.1	372.1 ± 3.7
octacontane	380.8 ± 3.5	379.2 ± 3.7	378.7 ± 4.1	379.6 ± 3.8
dooctacontane	388.5 ± 3.6	386.1 ± 3.7	387.1 ± 4.2	387.2 ± 3.8
tetraoctacontane	395.8 ± 3.6	393.8 ± 3.8	392.6 ± 4.3	394.0 ± 3.9
hexaoctacontane	403.7 ± 3.7	401.3 ± 3.9	401.5 ± 4.4	402.1 ± 4.0
octaoctancontane	411.3 ± 3.8	409.1 ± 4.0	407.4 ± 4.5	409.2 ± 4.1
nonacontane	418.9 ± 3.9	415.4 ± 4.0	415.0 ± 4.6	416.4 ± 4.3
dononacontane	426.1 ± 3.9	423.0 ± 4.1		424.5 ± 4.0

Figure 2. This figure plots the available vaporization enthalpies at $T = 298.15$ K of pentane on through to dononacontane as a function of the number of carbon atoms, N. Recommended literature values for pentane through to eicosane as a function of the number of carbon atoms were used to establish the relationship between vaporization enthalpy and carbon number, N. The results are quite linear and are represented by the following equation

$$\Delta_l^g H_m(298.15 \text{ K})/kJ \cdot mol^{-1} = (5.005 \pm 0.007)N +$$
$$(1.487 \pm 0.137); \quad N = (5 \text{ to } 20) \quad r^2 = 0.9999 \quad (4)$$

This relationship was used to generate the solid line in Figure 2. The values calculated using the program PERT2 are represented by the empty circles. These estimations fit the line generated by eq 4 within experimental error up to about hexacontane. Larger alkanes begin to diverge from the line, and the PERT2 model predicts substantial curvature. This curvature is consistent with expectations which are based on the observance of convergence between critical and boiling temperature as a function of the number of carbon atoms. Results from correlation−gas chromatography are also quantitatively consistent with the linear behavior predicted by eq 4 up to about hexacontane and then show the same divergence as predicted by PERT2. It should be emphasized that the vaporization enthalpies of all the alkanes larger than eicosane have been measured by correlation−gas chromatography and all are based on extrapolations using the recommended values of heptadecane to eicosane as standards. It is quite possible that the curvature observed in $\Delta_l^g H_m(298.15 \text{ K})$ measured by gas chromatography is simply an artifact of the extrapolations. As a test of this possibility, we recently reported the dependence of the enthalpy of transfer, measured by correlation−gas chromatography, as a function of the number of carbon atoms.[5] Enthalpies of transfer measurements are experimental measurements that are not based on extrapolation. The enthalpy of transfer, $\Delta_{sln}^g H_m(T_m)$, can be related to the vaporization enthalpy and the enthalpy of interaction of the analyte on the column, $\Delta_{sln} H_m(T_m)$, by the following thermodynamic relation

$$\Delta_{sln}^g H_m(T_m) = \Delta_l^g H_m(T_m) + \Delta_{sln} H_m(T_m) \quad (5)$$

As the length of the hydrocarbon chain increases, the critical and boiling temperatures are observed to converge. Consequently, the vaporization enthalpy at the normal boiling temperature should reach some maximum value and then decrease to zero. At temperatures below the normal boiling temperature, the vaporization enthalpy may not approach zero but is expected to show curvature.[5,9] A model consistent with the dependence of vaporization enthalpy with size is related to the type of interactions that may dominate in large molecules. As the size of the linear alkane increases, it can fold back on itself. With increasing size, the ratio of intermolecular interaction to intramolecular interaction decreases with chain length, N, and in the limit should approach zero. Using a sphere as a simple
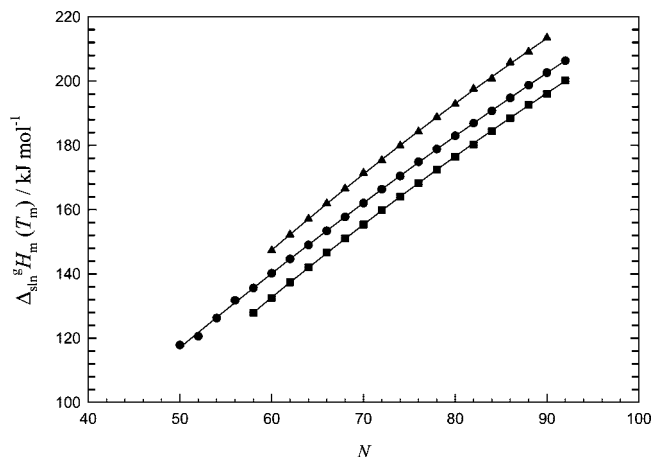
Figure 3. Enthalpies of transfer measured in this work as a function of the number of carbon atoms, N. The circles represent results from run 1, and the triangles represent the results of run 3. 5 kJ was arbitrarily subtracted from the results of run 2, squares, to separate these results from the results from run 1 for illustration in this figure. Fitting the experimental data to a second-order polynomial results in the following equations:

circles: $\Delta_{sln}^g H_m(676 \text{ K})/kJ \cdot mol^{-1} = -(5.64 \pm 0.56) \cdot$
$$10^{-3}N^2 + (2.93 \pm 0.08)N - (15.1 \pm 2.8);$$
$$r^2 = 0.9998 \quad (6)$$

squares: $\Delta_{sln}^g H_m(676 \text{ K})/kJ \cdot mol^{-1} = -(7.47 \pm 0.42) \cdot$
$$10^{-3}N^2 + (3.24 \pm 0.06)N - (29.8 \pm 2.3);$$
$$r^2 = 0.9999 \quad (7)$$

triangles: $\Delta_{sln}^g H_m(653 \text{ K})/kJ \cdot mol^{-1} = -(8.37 \pm 0.96) \cdot$
$$10^{-3}N^2 + (3.45 \pm 0.14)N - (29.6 \pm 5.3);$$
$$r^2 = 0.9998 \quad (8)$$

model, intermolecular interactions should show a dependence similar to the ratio of the surface area of a sphere to its internal volume as a function of the sphere's radius.

The enthalpy of transfer from the column to the gas phase depends on two terms, the vaporization enthalpy and the interaction of the material on the column, $\Delta_{sln} H_m(T_m)$, both measured at the mean temperature of measurement (eq 5). With increasing molecular size and linearity, both the vaporization enthalpy and the interaction of the material on the column should show the same dependence on size if the amount of folding of an alkane increases with increasing size.[5] Since enthalpies of transfer can be measured independent of any extrapolation, the behavior of $\Delta_{sln}^g H_m(T_m)$ as a function of size should be a more reliable indicator of the validity of the model. Recently, we reported the correlation of the enthalpies of transfer as a function of the number of carbon atoms from dotetracontane to hexaheptacontane.[5,9] While the relationship between N and $\Delta_{sln}^g H_m(T_m)$ could be fit quite satisfactorily by a linear function, a second-order polynomial with a slope that decreased with increasing size provided a better fit, consistent with the predictions of the model. This observation is similarly reproduced in plots of $\Delta_{sln}^g H_m(T_m)$ versus N for the larger alkanes as well. A corresponding plot of the enthalpies of transfer versus N measured for pentacontane to dononanontane is illustrated in Figure 3. As quantified by the parabolic polynomials eqs 6 to 8 provided below the figure, curvature is indeed observed; a maximum $\Delta_{sln}^g H_m(T_m)$ in the neighborhood of 225 carbons is suggested. The observed maximum would be expected to be dependent on temperature.[5]

Table 3. Vaporization Enthalpies of the *n*-Alkanes at *T* = 298.15 K as a Function of the Number of Carbon Atoms, *N*[a]

N	$\Delta_l^g H_m$(298.15 K) kJ·mol^{-1}	N	$\Delta_l^g H_m$(298.15 K) kJ·mol^{-1}	N	$\Delta_l^g H_m$(298.15 K) kJ·mol^{-1}	N	$\Delta_l^g H_m$(298.15 K) kJ·mol^{-1}
5	26.42	21	106.8 ± 2.6	36	182.8 ± 5.5	64	315.4 ± 2.9
6	31.52	22	111.9 ± 2.7	37	187.5 ± 5.6	66	324.0 ± 3.0
7	36.57	23	117.0 ± 2.8	38	192.5 ± 5.7[b]	68	331.9 ± 3.0
8	41.56	24	121.9 ± 2.8	40	203.5 ± 2.9	70	340.3 ± 3.1
9	46.55	25	126.8 ± 2.9	42	213.5 ± 2.1	72	348.4 ± 3.2
10	51.42	26	131.7 ± 3.3	44	223.7 ± 2.3	74	356.2 ± 3.3
11	56.58	27	135.6 ± 3.3	46	233.3 ± 2.3	76	364.3 ± 3.3
12	61.52	28	141.9 ± 5.1	48	243.0 ± 2.4	78	372.1 ± 3.7
13	66.68	29	147.1 ± 5.3	50	252.5 ± 2.5	80	379.6 ± 3.8
14	71.73	30	152.3 ± 5.3	52	261.8 ± 3.6	82	387.2 ± 3.8
15	76.77	31	157.2 ± 1.4[b]	54	271.0 ± 3.7	84	394.0 ± 3.9
16	81.35	32	162.5 ± 1.4	56	279.7 ± 3.8	86	402.2 ± 4.0
17	86.47	33	167.6 ± 1.4	58	288.5 ± 3.9	88	409.3 ± 4.1
18	91.44	34	172.7 ± 1.5	60	299.9 ± 3.0	90	416.5 ± 4.3
19	96.44	35	178.1 ± 5.4[b]	62	306.8 ± 2.8	92	424.5 ± 4.0
20	101.81						

[a] Values for *N* = 5 to *N* = 20 from ref 6. Uncertainties were calculated from the uncertainty associated with the slope and intercept and averaged over each run. [b] See ref 16.

Table 4. *A*, *B*, *C*, and *D* Coefficients of Equation 12 for Heneicosane to Dononacontane[a]

	$10^{-8}A$ / T^3	$10^{-6}B$ / T^2	C / T	D
heneicosane	1.9989	−2.9075	−98.135	6.6591
docosane	2.1713	−3.1176	110.72	6.5353
tricosane	2.3386	−3.322	310.77	6.4198
tetracosane	2.5072	−3.5286	530.15	6.282
pentacosane	2.6738	−3.7307	741.19	6.150
hexacosane	2.8244	−3.9193	910.53	6.070
heptacosane	3.0092	−4.1253	1198.8	5.811
octacosane	3.1389	−4.3120	1279.4	5.884
nonacosane	3.2871	−4.5043	1431.2	5.841
triacontane	3.4404	−4.6998	1601.6	5.770
hentriacontane	3.6037	−4.9002	1791.2	5.679
dotriacontane	3.7524	−5.0921	1947.2	5.630
tritriacontane	3.8983	−5.2809	2098.0	5.585
tetratriacontane	4.0435	−5.4679	2249.5	5.537
pentatriacontane	4.1746	−5.6480	2363.8	5.544
hexatriacontane	4.3320	−5.8432	2553.2	5.447
heptatriacontane	4.4890	−6.0370	2743.2	5.347
octatriacontane	4.6330	−6.2230	2891.9	5.304
tetracontane	4.9289	−6.6065	3183.3	5.270
dotetracontane	5.1471	−6.9224	3348.9	5.291
tetratetracontane	5.5011	−7.3467	3778.6	5.117
hexatetracontane	5.6451	−7.5992	3810.6	5.224
octatetracontane	5.8908	−7.9326	4039.6	5.187
pentacontane	6.1330	−8.2602	4268.3	5.143
dopentacontane	4.8707	−7.4087	1564.8	7.455
tetrapentacontane	5.0959	−7.7167	1772.4	7.410
hexapentacontane	5.3213	−8.0192	1997.2	7.326
octapentacontane	5.5446	−8.3203	2215.7	7.251
hexacontane	7.3061	−9.8448	5365.4	4.957
dohexacontane	6.1197	−9.0298	2863.7	7.000
tetrahexacontane	6.2051	−9.2215	2812.1	7.149
hexahexacontane	6.2905	−9.4126	2761.7	7.295
octahexacontane	6.3771	−9.5964	2731.5	7.398
heptacontane	6.4622	−9.7833	2688.6	7.527
doheptacontane	6.5473	−9.9677	2650.7	7.646
tetraheptacontane	6.6325	−10.1491	2619.6	7.750
hexaheptacontane	6.7165	−10.3320	2580.8	7.870
octaheptacontane	6.9185	−10.6352	2862.6	7.718
octacontane	7.0339	−10.8450	2927.0	7.731
dooctacontane	7.1142	−11.0100	2862.8	7.852
tetraoctacontane	7.2562	−11.2545	3066.0	7.726
hexaoctacontane	7.3278	−11.4184	2970.3	7.897
octaoctacontane	7.4656	−11.6595	3147.1	7.810
nonacontane	7.5587	−11.8287	3121.0	7.885
dononacontane	7.7815	−12.1830	4010.6	6.856

[a] The A, B, C, and D coefficients for heneicosane to hexaheptacontane taken from refs 1, 2, and 5.

B. Vapor Pressures. In addition to their usefulness in obtaining vaporization enthalpies, the slopes and intercepts provided in Table 1, runs 1 to 3, can also be used to evaluate vapor pressures, *p*, when used in combination with experimental data. The use of the retention time data to provide vapor pressure data has been described previously.[1,2,5] The equations associated with the slopes and intercepts of each compound relate the temperature dependence of the vapor pressure of the solute (t_o/t_a) above the stationary phase of the column over a narrow temperature range. Although these equations would not be expected to be accurate in predicting vapor pressures by themselves, when used in combination with a series of standards with known vapor pressures at the temperatures of interest, the results obtained by correlation have been shown to be satisfactory.[1,2] Vapor pressure equations for heneicosane to hexaheptacontane have previously been reported in the form of eq 9.[1,2,5] The *A*, *B*, *C*, and *D* coefficients of this equation are reported in Table 4. *T* represents the temperature and p_o = 101.325 kPa.

$$\ln(p/p_o) = A(T/\text{K})^{-3} + B(T/\text{K})^{-2} + C(T/\text{K})^{-1} + D \quad (9)$$

Values of $\ln(p/p_o)$ for the standards were calculated using eq 9 at each temperature over the temperature range *T* = (298.15 to 540) K at 30 K intervals. In the first correlation, $\ln(p/p_o)$ values using eq 9 and the appropriate constants of Table 4 were calculated for the *n*-alkane standards in Table 1 up to hexaheptacontane. The results were correlated with the corresponding $\ln(t_o/t_a)$ values calculated from the slopes and intercepts in Table 1 for both the standards and the alkanes whose values were being evaluated. For those alkanes being evaluated, t_o/t_a values for each run were first averaged, and $\ln(t_o/t_a)_{average}$ was then correlated with $\ln(p/p_o)$. The results of this correlation are illustrated in Table 5 at *T* = 298.15 K by eq 10 given at the bottom of the table. Similar correlations were repeated at 30 K intervals. From the linear correlations obtained, it was possible to calculate $\ln(p/p_o)$ values for all the target alkanes at each temperature over the temperature range *T* = (298.15 to 540) K. Values of $\ln(p/p_o)$ and $\ln(t_o/t_a)$ were always highly correlated. Once $\ln(p/p_o)$ values were evaluated at each temperature over this range, the values of $\ln(p/p_o)$ were plotted against 1/*T* and the results fitted to eq 9. The constants obtained for eq 9 for octaheptacontane to dononacontane are also included in Table 4.

As noted above, there are no experimental values of vapor pressure and vaporization enthalpy available to our knowledge with which to compare these results. As a consequence of the

Table 5. Evaluation of the Vapor Pressures of the Even Alkanes from Octaheptacontane to Dononacontane at $T = 298.15$ K for Runs 1 to 3

$T = 298.15$ K	slope (T/K)	intercept	$\ln(t_o/t_a)$	$\ln(t_o/t_a)_{avg}$	$\ln(p/p_o)$ lit.[1]	$\ln(p/p_o)$ calc
pentacontane	−14177	23.047		−24.50	−50.3	−50.7
dopentacontane	−14507	23.277		−25.38	−52.3	−52.0
tetrapentacontane	−15180	24.022		−26.89	−54.2	−54.2
hexapentacontane	−15851	24.763		−28.40	−56.1	−56.5
octapentacontane	−16308	25.187		−29.51	−58.0	−58.1
hexacontane	−16862	25.755	−30.8			
	−16538	25.404	−30.07			
	−17445	26.708	−31.8	−30.66	−60.2	−59.8
dohexacontane	−17397	26.299	−32.05			
	−17131	26.037	−31.42			
	−18030	27.347	−33.13	−31.98	−61.9	−61.8
tetrahexacontane	−17919	26.824	−33.28			
	−17686	26.614	−32.71			
	−18610	27.979	−34.44	−33.25	−63.7	−63.6
hexahexacontane	−18449	27.364	−34.52			
	−18235	27.182	−33.98			
	−19185	28.603	−35.74	−34.51	−65.6	−65.5
octahexacontane	−18968	27.887	−35.73			
	−18763	27.722	−35.21			
	−19734	29.189	−37	−35.74	−67.3	−67.3
heptacontane	−19487	28.411	−36.95			
	−19287	28.256	−36.43			
	−20309	29.816	−38.3	−36.97	−69.1	−69.1
doheptacontane	−20005	28.935	−38.16			
	−19830	28.819	−37.69			
	−20771	30.271	−39.39	−38.2	−70.9	−71.0
tetraheptacontane	−20501	29.429	−39.33			
	−20338	29.334	−38.88			
	−21312	30.847	−40.63	−39.39	−72.6	−72.7
hexaheptacontane	−21031	29.973	−40.57			
	−20844	29.844	−40.07			
	−21833	31.396	−41.83	−40.59	−74.4	−74.5
octaheptacontane	−21512	30.445	−41.71			
	−21347	30.353	−41.25			
	−22364	31.959	−43.05	−41.76		−76.2
octacontane	−22009	30.942	−42.87			
	−21828	30.829	−42.38			
	−22846	32.449	−44.18	−42.91		−77.9
dooctacontane	−22481	31.406	−43.99			
	−22282	31.269	−43.47			
	−23408	33.064	−45.45	−44.02		−79.6
tetraoctacontane	−22935	31.842	−45.08			
	−22783	31.775	−44.64			
	−23781	33.387	−46.37	−45.14		−81.2
hexaoctacontane	−23424	32.331	−46.23			
	−23272	32.269	−45.79			
	−24378	34.059	−47.71	−46.3		−82.9
octaoctancontane	−23898	32.801	−47.35			
	−23779	32.789	−46.97			
	−24775	34.423	−48.67	−47.44		−84.6
nonacontane	−24371	33.269	−48.47			
	−24189	33.166	−47.97			
	−25289	34.969	−49.85	−48.5		−86.2
dononacontane	−24814	33.695	−49.53			
	−24684	33.669	−49.12	−49.31		−87.4

$$\ln(p/p_o)_{calc} = (1.480 \pm 0.012)\ln(t_o/t_a) - (14.43 \pm 0.22) \quad r^2 = 0.9992$$

lack of other experimental data, we have compared vapor pressures and vaporization enthalpies at $T = 298.15$ K with those predicted by PERT2 and vapor pressures at temperatures at which the Antoine Constants estimated by Kudchadker and Zwolinski and PERT2 were applicable. These comparisons are summarized in Table 6. As noted previously, both vapor pressures and vaporization enthalpies calculated at $T = 298.15$ K by PERT2 (columns 3 and 5, respectively) are in good agreement with the results of this work (columns 2 and 4) up to about C_{60}. Above hexacontane, the two results begin to diverge. Vaporization enthalpy values calculated by PERT2 above C_{60} increase more slowly and as a consequence, higher

vapor pressures are predicted in comparison to the results obtained by correlation-gas chromatography.

It should be noted that the vaporization enthalpies reported in column 4 of Table 6 at $T = 298.15$ K were obtained by direct correlation of $\Delta_{sln}{}^g H_m(T_m)$ with $\Delta_l{}^g H_m(298.15 \text{ K})$ (Table 1). The vaporization enthalpies calculated at T_m, column 9 of Table 6, were calculated using eq 9 and the constants of Table 4. Vaporization enthalpies using eq 9 were calculated at $T = T_m$ as the negative product of the slope of the line and gas constant generated from plots of $\ln(p/p_o)$ vs $1/T$ over a $T = 30$ K range. Use of eq 9 to calculate vaporization enthalpies at $T = 298.15$ K provided slightly different vaporization enthalpies than those
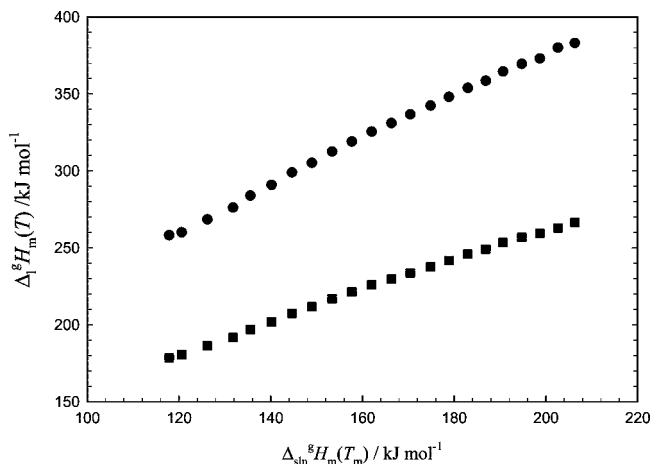
Figure 4. Plots of vaporization enthalpies calculated by PERT2 against enthalpies of transfer measured for run 1. Circles, $T = 298.15$ K; squares, $T = 500$ K. The lines calculated by linear regression and by using a second-order polynomial are given by

circles:
$$\Delta_l^g H_m(298.15\ \text{K})/\text{kJ}\cdot\text{mol}^{-1} =$$
$$(1.46 \pm 0.011)\Delta_{\text{sln}}^g H_m(676\ \text{K}) + (60.56 \pm 1.36\,);$$
$$r^2 = 0.9977 \quad (10)$$

$$\Delta_l^g H_m(298.15\ \text{K})/\text{kJ}\cdot\text{mol}^{-1} = -(2.58 \pm 0.33)\cdot$$
$$10^{-3}\Delta_{\text{sln}}^g H_m(676\ \text{K}) + (2.28 \pm 0.11)\Delta_{\text{sln}}^g H_m(676\ \text{K}) +$$
$$(22.3 \pm 8.59\,); \quad r^2 = 0.9994 \quad (11)$$

squares:
$$\Delta_l^g H_m(500\ \text{K})/\text{kJ}\cdot\text{mol}^{-1} =$$
$$(1.008 \pm 0.011)\Delta_{\text{sln}}^g H_m(676\ \text{K}) + (60.56 \pm 1.36\,);$$
$$r^2 = 0.9977 \quad (12)$$

$$\Delta_l^g H_m(500\ \text{K})/\text{kJ}\cdot\text{mol}^{-1} = -(1.82 \pm 0.2)\cdot$$
$$10^{-3}\Delta_{\text{sln}}^g H_m(676\ \text{K}) + (1.60 \pm 0.06)\Delta_{\text{sln}}^g H_m(676\ \text{K}) +$$
$$(14.0 \pm 5.1\,); \quad r^2 = 0.9996 \quad (13)$$

reported in the fourth column of this table. The standard deviation between vaporization enthalpies evaluated directly as in Table 1 and those evaluated using eq 9 and the constants in Table 4 was ($\pm$ 1.57) kJ·mol^{-1}. All vaporization enthalpies calculated by using eq 9 were slightly larger than those obtained by direct correlation of $\Delta_{\text{sln}}^g H_m(T_m)$ with $\Delta_l^g H_m(298.15\ \text{K})$ except for two that were slightly smaller. The largest deviations were observed for the largest alkanes studied, those for which the extrapolations are the most extensive. The largest difference was 5.7 kJ·mol^{-1} observed for octaoctacontane. The dashed line and the solid circles in Figure 2 illustrate this deviation. The dashed line represents vaporization enthalpies calculated using eq 9, and the solid circles represent average values calculated using eqs 1 to 3. The two sets of results are probably still within experimental error of each other. The differences are probably a good indication of the magnitude of the absolute error in the values, and relative errors between homologues are probably less.

Since the vaporization enthalpies reported in column 9 of Table 6 were calculated at T_m using eq 9, a question arises regarding the divergence in $\Delta_l^g H_m(T_m)$ observed in Figure 2 between these results and those calculated using PERT2 both at $T = 298.15$ K and T_m. Is this divergence a consequence of the deviations just discussed and/or due to the extensive
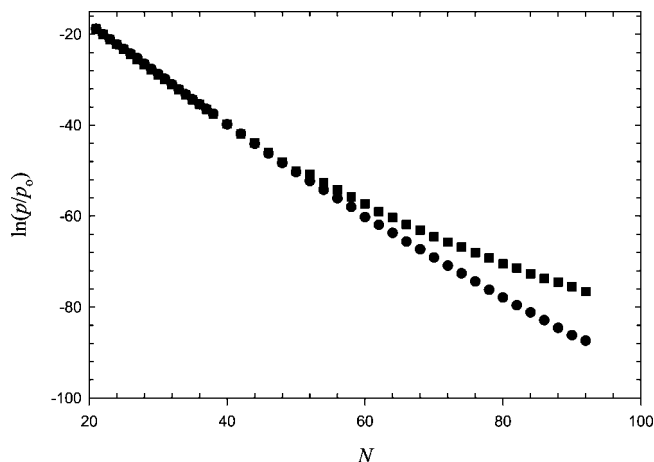
Figure 5. Plots of $\ln(p/p_o)$ against the number of carbon atoms, N, at $T = 298.15$ K. The circles are values calculated by correlation gas chromatography (eq 9), and the squares are values calculated by PERT2. Both results show varying amounts of curvature. The curves are fit by the following relationships

circles: $\ln(p/p_o) = (2.77 \pm 0.05)10^{-3}N^2 -$
$$(1.285 \pm 0.005)N + (7.21 \pm 0.1.4\,); \quad r^2 = 0.9999 \quad (14)$$

squares: $\ln(p/p_o) = (5.79 \pm 0.10)10^{-3}N^2 -$
$$(1.47 \pm 0.01)N + (9.69 \pm 0.27\,); \quad r^2 = 0.9998 \quad (15)$$
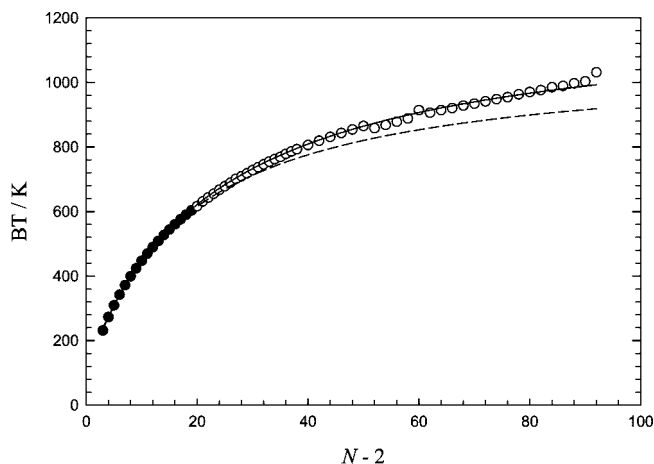
Figure 6. Plot of the normal boiling temperatures, BT, of the *n*-alkanes as a function of the number of methylene groups; N = the number of carbon atoms. The solid circles represent the experimental boiling temperatures of propane to eicosane. The empty circles are boiling temperatures calculated by correlation gas chromatography using eq 9 and the constants of Table 4. The dotted line was calculated for the *n*-alkanes using a limiting boiling temperature of $T_B(\infty) = 1076$ K and eq 16a. This limiting boiling temperature was generated by fitting the experimental data to a hyperbolic function as described in the text. The solid line was obtained by using a value of $T_B(\infty) = 1217$ K obtained by averaging $T_B(\infty)$ of a series of homologous compounds that each approach the structure of polyethylene in the limit. This resulted in eq 16b.[17]

extrapolations associated with this work? To address this question, the following correlations were performed. It has previously been demonstrated that vaporization enthalpies of hydrocarbons correlate linearly with enthalpies of transfer measured by gas chromatography.[1–5] This linear correlation has normally been demonstrated at $T = 298.15$ K since this generally has been the temperature of interest. The choice in temperature, however, is arbitrary. Correlation between $\Delta_{\text{sln}}^g H_m(T_m)$ and $\Delta_l^g H_m(T)$ should be observed at any value of T, provided the

Table 6. Comparison of Vaporization Enthalpies and Vapor Pressures of This Work With Estimated Values

| | $\ln(p/p_o)$ | | $\Delta_l^g H_m(298\ K)$ | | T_m | $\ln(p/p_o)$ | | $\Delta_l^g H_m(T_m/K)$ | | |
| | $T = 298.15\ K$ | | $kJ\cdot mol^{-1}$ | | | $T = T_m$ | | $kJ\cdot mol^{-1}$ | | |
	This work	PERT2	This work	PERT2	K	This work	ref 15	This work	ref 15	PERT2
heneicosane	−18.8	−18.8	106.8	107.8	437	−6.4	−6.4	86.7	88.3	85.0
docosane	−20.0	−20.0	111.9	113.8	443	−6.6	−6.4	90.7	91.8	88.1
tricosane	−21.1	−21.1	117.0	118.4	455	−6.5	−6.5	91.3	93.9	90.3
tetracosane	−22.2	−22.2	121.9	123.7	463	−6.5	−6.5	93.2	94.6	93.1
pentacosane	−23.2	−23.3	126.8	128.9	472	−6.5	−6.5	96.4	99.1	95.5
hexacosane	−24.3	−24.4	131.7	134.2	481	−6.4	−6.5	97.5	101.4	97.8
heptacosane	−25.2	−25.6	135.6	139.5	488	−6.5	−6.5	99.1	104.1	100.4
octadocosane	−26.5	−26.7	141.9	144.7	496	−6.5	−6.5	102.2	106.4	102.7
nonacosane	−27.6	−27.8	147.1	150.1	503	−6.5	−6.5	104.7	108.9	104.0
triacontane	−28.7	−28.9	152.3	155.4	510	−6.6	−6.6	107.0	111.2	107.5
hentriacontane	−29.8	−30.0	157.3	160.6	518	−6.5	−6.5	109.7	113.7	109.6
dotriacontane	−31.0	−31.1	162.5	165.9	525	−6.5	−6.5	111.9	115.8	111.8
tritriacontane	−32.1	−32.2	167.6	171.2	532	−6.5	−6.5	113.3	117.9	114.0
tetratriacontane	−33.2	−33.3	172.7	176.4	538	−6.6	−6.5	115.5	120.2	116.2
pentatriacontane	−34.3	−34.4	178.0	181.7	544	−6.6	−6.6	117.9	122.2	118.4
hexatriacontane	−35.4	−35.4	182.8	186.9	550	−6.6	−6.6	119.8	124.3	120.5
heptatriacontane	−36.4	−36.5	187.5	192.1	556	−6.6	−6.6	121.6	126.2	122.5
octatriacontane	−37.5	−37.6	192.6	197.3	561	−6.7	−6.6	123.8	128.4	124.7
tetracontane	−39.8	−39.7	203.5	207.7	572	−6.7	−6.6	128.1	132.2	128.7
dotetracontane	−41.9	−41.9	213.5	218	582	−6.8	−6.6	132.1	136	132.7
tetratetracontane	−44.1	−43.9	223.7	228.1	592	−6.8	−6.6	135.9	139.3	136.4
hexatetacontane	−46.2	−46	233.3	238.2	601	−6.9	−6.6	139.7	142.8	140.2
octatetracontane	−48.3	−48.1	243	248.2	610	−6.9	−6.6	143.2	145.9	143.8
pentacontane	−50.3	−50.1	252.5	258.1	618	−7	−6.6	146.8	149	147.4
dopentacontane	−52.3	−50.8	261.8	260	626	−7	−6.6	152.8	152	147.5
tetrapentacontane	−54.2	−52.6	270.9	268.4	633	−7	−6.6	156.3	155	150.5
hexapentacontane	−56.1	−54.2	279.6	276.1	640	−7.1	−6.6	159.4	157.8	153.0
octapentacontane	−58	−55.8	288.3	283.9	647	−7.2	−6.6	162.4	160.3	155.5
hexacontane	−60.2	−57.3	299.9	290.8	653	−7.3	−6.6	163.4	163	157.8
dohexacontane	−61.9	−59	306.7	299	660	−7.3	−6.6	168.7	165.2	160.4
tetrahexacontane	−63.7	−60.3	315.3	305.2	665	−7.4	−6.7	172.3	168.3	162.4
hexahexacontane	−65.6	−61.8	323.9	312.5	671	−7.4	−6.6	175.5	170	164.7
octahexacontane	−67.3	−63.1	331.9	319	676	−7.5	−6.6	178.6	172.3	166.7
heptacontane	−69.1	−64.5	340.1	325.5	681	−7.6	−6.6	180.6	174.4	168.8
doheptacontane	−70.9	−65.7	348.2	331	686	−7.6	−6.6	184.9	176.4	170.3
tetraheptacontane	−72.6	−66.8	356.1	336.6	691	−7.7	−6.6	187.8	178.2	171.8
hexaheptacontane	−74.4	−68.0	364.2	342.3	695	−7.8	−6.6	192.2	180.4	173.6
octaheptacontane	−76.2	−69.2	372.1	348	700	−7.9	−6.6	193.7	181.6	175.2
octacontane	−77.9	−70.5	379.6	353.8	704	−8	−6.6	196.5	183.4	177.0
dooctacontane	−79.6	−71.4	387.2	358.5	708	−8.1	−6.6	199.4	185.1	178.3
tetraoctacontane	−81.2	−72.7	394.1	364.5	711	−8.2	−6.7	202.0	187.1	180.4
hexaoctacontane	−82.9	−73.7	402.2	369.4	715	−8.3	−6.6	205.2	188.4	181.7
octaoctacontane	−84.6	−74.5	409.3	373.0	718	−8.4	−6.7	207.8	190.2	182.6
nonacontane	−86.2	−75.5	416.5	380.0	722	−8.5	−6.6	210.4	191.4	183.9
dononacontane	−87.4	−76.6	425.5	383.0	725	−8.7	−6.6	209.2	192.8	185.5

vaporization enthalpies of the reference compounds are all available at the same reference temperature, T. To determine whether the divergence observed at both $T = 298.15$ K and T_m between the two sets of values in Table 6 is real or simply an artifact of the extrapolations involved in this work, the experimental enthalpies of transfer measured at $T_m = 676$ K, run 1, were correlated with the vaporization enthalpies calculated by PERT2 at $T = (298.15$ and $500)$ K. If the vaporization enthalpies calculated by PERT2 are indeed accurate, then the experimental enthalpies of transfer of the larger alkanes, which have shown curvature with N (Figure 3), should correlate linearly with the results of PERT2; otherwise, some curvature should be observed.

Figure 4 illustrates the nature of the two correlations obtained. The results at both temperatures are fit quite satisfactorily by a linear correlation. However, some curvature is indeed observed as suggested by the quality of the fit, r^2, described in the caption of the figure by the linear and parabolic functions, eqs 10 to 13. Results with similar curvature were also observed for runs 2 and 3 (not shown). The enthalpy of transfer measurements suggests that the curvature observed using PERT2 may be somewhat exaggerated.

A similar trend is observed in $\ln(p/p_o)$ values calculated by correlation gas chromatography and PERT2. Figure 5 illustrates the behavior of $\ln(p/p_o)$ versus N. As with vaporization enthalpies, these results suggest that the amount of curvature obtained in this study, eqs 14 and 15, as a function of the number of carbon atoms, N, is slightly less than predicted by PERT2.

As a test of how well eq 9 extrapolates with temperature, the normal boiling temperatures of heneicosane to dononacontane were predicted using the constants of Table 4. Figure 6 illustrates the results. The solid circles represent the experimental boiling temperatures of propane through to eicosane. The empty circles represent the boiling temperatures predicted by eq 9 and the constants of Table 4. The dotted line was obtained by fitting the experimental boiling temperatures for the n-alkanes from C_3 to C_{20} with a hyperbolic function, eq 16a.[17] In this equation, T_B represents the normal boiling temperature; $T_B(\infty)$ is the limiting temperature when the number of methylene groups of the n-alkane, $(N$-2$)$, approaches infinity; and a_B and b_B are the slope and intercept of the equation of the best straight line obtained when plotting the function $1/[1 - T_B/T_B(\infty)]$ vs N-2 and allowing $T_B(\infty)$ to vary. Eq 16b was previously reported by averaging $T_B(\infty)$ obtained from similar plots of a series of

homologous *n*-alkane derivatives that also approach polyethylene in the limit.[17] The constants a_{Bm} and b_{Bm} were the slope and intercept generated using this averaged limiting temperature, $T_B(\infty) = 1217$, in plots of $1/[1 - T_B/T_B(\infty)]$ vs *N*-2 for the *n*-alkane derivatives.

$$T_B = T_B(\infty)(1 - 1/(a_B(N\text{-}2) + b_B)) \qquad (16)$$

$$T_B(\infty) = 1076; \ a_B = 0.06231; \ b_B = 1.214 \qquad (16a)$$

$$T_B(\infty) = 1217; \ a_{Bm} = 0.04694; \ b_{Bm} = 1.1984 \qquad (16b)$$

As illustrated in the figure, the fit between the boiling temperatures generated by extrapolation of eq 9 and those obtained by extrapolation of fitted experimental data is remarkably good considering the hypothetical nature of both comparisons.

Summary

The vaporization enthalpies and vapor pressures of the even *n*-alkanes from eicosane to dononacontane are evaluated through a process of extrapolation by correlation−gas chromatography. The vaporization enthalpies of all these hydrocarbons are measurements of the subcooled liquid and as such are hypothetical properties. The results are compared to two sets of estimated values. The results are generally in good agreement up to approximately hexacontane. Above hexacontane, the estimated and measured values begin to diverge. However both experimental and estimation methods are in agreement with the prediction that vaporization enthalpies of linear molecules will show some curvature and with increasing size at temperatures below boiling. The boiling temperatures predicted by extrapolation of the vapor pressure equations generated by correlation gas chromatography are in remarkably good agreement with boiling temperature predictions generated by extrapolated experimental data.

Acknowledgment

Supporting Information Available:

Tables including the experimental retention times described in the text. This material is available free of charge via the Internet at http://pubs.acs.org.

Literature Cited

(1) Chickos, J. S.; Hanshaw, W. Vapor pressures and vaporization enthalpies of the n-alkanes from C$_{31}$ to C$_{38}$ at *T* = 298.15 K by correlation gas chromatography. *J. Chem. Eng. Data* **2004**, *49*, 620–30.

(2) Chickos, J. S.; Hanshaw, W. Vapor pressures and vaporization enthalpies of the n-alkanes from C$_{21}$-C$_{30}$ at *T* = 298.15 K by correlation-gas chromatography. *J. Chem. Eng. Data* **2004**, *49*, 77–85.

(3) Chickos, J. S.; Webb, P.; Nichols, G.; Kiyobayashi, T.; Cheng, P.-C.; Scott, L. The enthalpy of vaporization and sublimation of corannulene, coronene, and perylene at *T* = 298.15 K. *J. Chem. Thermodyn.* **2002**, *34*, 1195–1206.

(4) Chickos, J. S.; Hesse, D.; Hosseini, S.; Nichols, G.; Webb, P. Sublimation enthalpies at 298.15 K using correlation gas chromatography and differential scanning calorimetry measurements. *Thermochim. Acta* **1998**, *313*, 101–110.

(5) Chickos, J. S.; Wang, T.; Sharma, E. Hypothetical Thermodynamic Properties: Vapor pressures and vaporization enthalpies of the even n-alkanes from C$_{40}$ to C$_{76}$ at *T* = 298.15 K by Correlation-gas chromatography. Are the vaporization enthalpies a linear function of carbon number. *J. Chem. Eng. Data* **2008**, *53*, 481–91.

(6) Ruzicka, K.; Majer, V. Simultaneous treatment of vapor pressures and related thermal data between the triple point and normal boiling temperatures for n-alkanes C$_5$-C$_{20}$. *J. Phys. Chem. Ref. Data* **1994**, *23*, 1–39.

(7) Zhao, H.; Unhannanant, P.; Hanshaw, W.; Chickos, J. S. The enthalpies of vaporization and vapor pressures of some deuterated hydrocarbons. Liquid vapor pressure isotope effects. *J. Chem. Eng. Data* **2008**, *53*, 1545–1556.

(8) Hanshaw, W.; Nutt, M.; Chickos, J. S. Hypothetical thermodynamic properties. Subcooled vaporization enthalpies and vapor pressures of polyaromatic hydrocarbons. *J. Chem. Eng. Data* **2008**, in press.

(9) At the critical temperature, the vaporization enthalpy vanishes. The critical pressure is also observed to decrease with size and can be modeled to approach 1 atm pressure. Chickos, J. S. Hypothetical Thermodynamic properties: The boiling and critical temperature of polyethylene and polytetrafluoroethylene. *J. Chem. Eng. Data* **2004**, *49*, 518–526.

(10) Morgan, D. L.; Kobayashi, R. Extension of Pitzer CSP models for vapor pressures and heats of vaporization to long chain hydrocarbons. *Fluid Phase Equilib.* **1994**, *94*, 51–87.

(11) PERT 2 is a FORTRAN program written by D L. Morgan in 1996 which includes parameters (critical temperature and pressure, T_c, P_c, acentric factor, normal boiling and melting temperature) for *n*-alkanes from C1 to C100 and heat of vaporization and vapor pressure correlations. The parameters for C$_{51}$ to C$_{100}$ are unpublished based on the critical property (T_c, P_c) correlations of Twu[12] and the Kudchadker & Zwolinski[13] extrapolation of *n*-alkane normal boiling temperature (NBT) presented in Zwolinski & Wilhoit (1971).[14] Acentric factors were calculated from estimated NBT, T_c, and P_c by using the PERT2 vapor pressure correlation. Morgan, D.L., Extension of Corresponding States Correlations using New Vapor Pressure Measurements of the n-Alkanes C$_{10}$ to C$_{28}$, Ph.D. Thesis, Rice University, Houston, TX 1990. Current address: David L. Morgan, Dow Corning Corporation, P.O. Box 994, M/S C043D1, Midland, MI 48686, Email Address: d.l.morgan@dowcorning.com; morganda@tm.net.

(12) Twu, C. H. An internally consistent correlation for predicting the critical properties and molecular weight of petroleum and coal-tar liquids. *Fluid Phase Equilib.*, **1984**, *16*, 137−150.

(13) Kudchadker, A. P.; Zwolinski, B. J. Vapor Pressures and Boiling Points of Normal Alkanes, C$_{21}$ to C$_{100}$. *J. Chem. Eng. Data* **1966**, *11*, 253–55.

(14) Zwolinski, B. J., and Wilhoit, R. C. *Handbook of vapor pressures and heats of vaporization of hydrocarbons and related compounds*; API44-TRC publication No. 101, Thermodynamics Research Center: TX 77843, 1971.

(15) Stephenson, R. M.; Malanowski, S. *Handbook of the Thermodynamics of Organic Compounds;* Elsevier: New York, 1987.

(16) These values differ slightly (± 0.2 or less) from the values reported in reference 1 due to an error reported in Table 3 for C$_{31}$ to C$_{38}$. The values reported for $\Delta_{sln}^g H_m(549.7)$ in reference 1 are in error. The correct values can be calculated from Table 2 (C$_{31}$ to C$_{38}$, reference 1) as the product of the negative slope of the line and the gas constant. The correct correlation equation listed under C$_{31}$ to C$_{38}$ in Table 3 of reference 1 should read: $\Delta^g H_m(298.15 \text{ K})/\text{kJ}\cdot\text{mol}^{-1} = (1.862 \pm 0.053)\Delta_{sln}^g H_m(549.7 \text{ K}) - (9.49 \pm 0.32)]$, $r^2 = 0.9984$. While the changes in the values for C$_{31}$, C$_{35}$, and C$_{38}$ affected subsequent correlations using these compounds as standards, the effect was small. The same mean value was obtained for all other compounds calculated using these compounds as standards when each respective value was rounded to one significant figure following the decimal. Consequently there are no further numerical effects on subsequent correlations.

(17) Chickos, J. S. Hypothetical thermodynamic properties: The boiling and critical temperature of polyethylene and polytetrafluoroethylene. *J. Chem. Eng. Data* **2004**, *49*, 518–26.